

Chapter 4

Local stability

(R. Mainieri and P. Cvitanović)

SO FAR we have concentrated on description of the trajectory of a single initial point. Our next task is to define and determine the size of a *neighborhood* of $x(t)$. We shall do this by assuming that the flow is locally smooth, and describe the local geometry of the neighborhood by studying the flow linearized around $x(t)$. Nearby points aligned along the stable (contracting) directions remain in the neighborhood of the trajectory $x(t) = f^t(x_0)$; the ones to keep an eye on are the points which leave the neighborhood along the unstable directions. As we shall demonstrate in chapter 18, in hyperbolic systems what matters are the expanding directions. The repercussion are far-reaching: As long as the number of unstable directions is finite, the same theory applies to finite-dimensional ODEs, state space volume preserving Hamiltonian flows, and dissipative, volume contracting infinite-dimensional PDEs.

4.1 Flows transport neighborhoods



As a swarm of representative points moves along, it carries along and distorts neighborhoods. The deformation of an infinitesimal neighborhood is best understood by considering a trajectory originating near $x_0 = x(0)$ with an initial infinitesimal displacement $\delta x(0)$, and letting the flow transport the displacement $\delta x(t)$ along the trajectory $x(x_0, t) = f^t(x_0)$.

4.1.1 Instantaneous shear

The system of linear *equations of variations* for the displacement of the infinitesimally close neighbor $x + \delta x$ follows from the flow equations (2.6) by Taylor

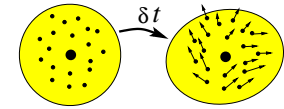


Figure 4.1: A swarm of neighboring points of $x(t)$ is instantaneously sheared by the action of the stability matrix A - a bit hard to draw.

expanding to linear order

$$\dot{x}_i + \delta \dot{x}_i = v_i(x + \delta x) \approx v_i(x) + \sum_j \frac{\partial v_i}{\partial x_j} \delta x_j.$$

The infinitesimal displacement δx is thus transported along the trajectory $x(x_0, t)$, with time variation given by

$$\frac{d}{dt} \delta x_i(x_0, t) = \sum_j \left. \frac{\partial v_i}{\partial x_j}(x) \right|_{x=x(x_0, t)} \delta x_j(x_0, t). \quad (4.1)$$

As both the displacement and the trajectory depend on the initial point x_0 and the time t , we shall often abbreviate the notation to $x(x_0, t) \rightarrow x(t) \rightarrow x$, $\delta x_i(x_0, t) \rightarrow \delta x_i(t) \rightarrow \delta x$ in what follows. Taken together, the set of equations

$$\dot{x}_i = v_i(x), \quad \delta \dot{x}_i = \sum_j A_{ij}(x) \delta x_j \quad (4.2)$$

governs the dynamics in the tangent bundle $(x, \delta x) \in \mathbf{TM}$ obtained by adjoining the d -dimensional tangent space $\delta x \in T\mathcal{M}_x$ to every point $x \in \mathcal{M}$ in the d -dimensional state space $\mathcal{M} \subset \mathbb{R}^d$. The *stability matrix* (velocity gradients matrix)

$$A_{ij}(x) = \frac{\partial v_i(x)}{\partial x_j} \quad (4.3)$$

describes the instantaneous rate of shearing of the infinitesimal neighborhood of $x(t)$ by the flow, figure 4.1.

Example 4.1 Rössler and Lorenz flows, linearized: (continued from example 3.6) For the Rössler (2.17) and Lorenz (2.12) flows the stability matrices are, respectively

$$A_{Ross} = \begin{pmatrix} 0 & -1 & -1 \\ 1 & a & 0 \\ z & 0 & x-c \end{pmatrix}, \quad A_{Lor} = \begin{pmatrix} -\sigma & \sigma & 0 \\ \rho-z & -1 & x \\ y & x & -b \end{pmatrix}. \quad (4.4)$$

(continued in example 4.6)

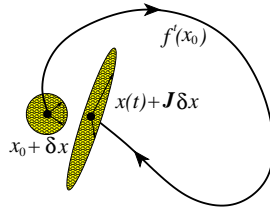


Figure 4.2: The Jacobian matrix J^t maps an infinitesimal displacement at x_0 into a displacement rotated and sheared by the linearized flow Jacobian matrix $J^t(x_0)$ finite time t later.

4.1.2 Linearized flow

Taylor expanding a *finite time* flow to linear order,

$$f_i^t(x_0 + \delta x) = f_i^t(x_0) + \sum_j \frac{\partial f_i^t(x_0)}{\partial x_{0j}} \delta x_j + \dots, \quad (4.5)$$

one finds that the linearized neighborhood is transported by

$$\delta x(t) = J^t(x_0) \delta x_0, \quad J_{ij}^t(x_0) = \left. \frac{\partial x_i(t)}{\partial x_j} \right|_{x=x_0}. \quad (4.6)$$

This Jacobian matrix is sometimes referred to as the *fundamental solution matrix* or simply *fundamental matrix*, a name inherited from the theory of linear ODEs. It is also sometimes called the *Fréchet derivative* of the nonlinear mapping $f^t(x)$. It is often denoted Df , but for our needs (we shall have to sort through a plethora of related Jacobian matrices) matrix notation J is more economical. J describes the deformation of an infinitesimal neighborhood at finite time t in the co-moving frame of $x(t)$.

As this is a deformation in the linear approximation, one can think of it as a deformation of an infinitesimal sphere enveloping x_0 into an ellipsoid around $x(t)$, described by the eigenvectors and eigenvalues of the Jacobian matrix of the linearized flow, figure 4.2. Nearby trajectories separate along the *unstable directions*, approach each other along the *stable directions*, and change their distance along the *marginal directions* at a rate slower than exponential, corresponding to the eigenvalues of the Jacobian matrix with magnitude larger than, smaller than, or equal 1. In the literature adjectives *neutral* or *indifferent* are often used instead of ‘marginal,’ (attracting) stable directions are sometimes called ‘asymptotically stable,’ and so on.

One of the preferred directions is what one might expect, the direction of the flow itself. To see that, consider two initial points along a trajectory separated by infinitesimal flight time δt : $\delta x_0 = f^{\delta t}(x_0) - x_0 = v(x_0) \delta t$. By the semigroup property of the flow, $f^{t+\delta t} = f^{\delta t+t}$, where

$$f^{\delta t+t}(x_0) = \int_0^{\delta t+t} d\tau v(x(\tau)) = \delta t v(x(t)) + f^t(x_0).$$

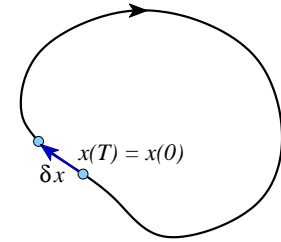


Figure 4.3: Any two points along a periodic orbit p are mapped into themselves after one cycle period T , hence a longitudinal displacement $\delta x = v(x_0) \delta t$ is mapped into itself by the cycle Jacobian matrix J_p .

Expanding both sides of $f^t(f^{\delta t}(x_0)) = f^{\delta t}(f^t(x_0))$, keeping the leading term in δt , and using the definition of the Jacobian matrix (4.6), we observe that $J^t(x_0)$ transports the velocity vector at x_0 to the velocity vector at $x(t)$ at time t :

$$v(x(t)) = J^t(x_0) v(x_0). \quad (4.7)$$

In nomenclature of page 71, the Jacobian matrix maps the initial, Lagrangian coordinate frame into the current, Eulerian coordinate frame.

The velocity at point $x(t)$ in general does not point in the same direction as the velocity at point x_0 , so this is not an eigenvalue condition for J^t ; the Jacobian matrix computed for an arbitrary segment of an arbitrary trajectory has no invariant meaning.

As the eigenvalues of finite time J^t have invariant meaning only for periodic orbits, we postpone their interpretation to chapter 5. However, already at this stage we see that if the orbit is periodic, $x(T_p) = x(0)$, at any point along cycle p the velocity v is an eigenvector of the Jacobian matrix $J_p = J^{T_p}$ with a unit eigenvalue,

$$J_p(x) v(x) = v(x), \quad x \in \mathcal{M}_p. \quad (4.8)$$

Two successive points along the cycle separated by δx_0 have the same separation after a completed period $\delta x(T_p) = \delta x_0$, see figure 4.3, hence eigenvalue 1.

As we started by assuming that we know the equations of motion, from (4.3) we also know stability matrix A , the instantaneous rate of shear of an infinitesimal neighborhood $\delta x_i(t)$ of the trajectory $x(t)$. What we do not know is the finite time deformation (4.6).

Our next task is to relate the stability matrix A to Jacobian matrix J^t . On the level of differential equations the relation follows by taking the time derivative of (4.6) and replacing $\dot{\delta x}$ by (4.2)

$$\dot{\delta x}(t) = J^t \delta x_0 = A \delta x(t) = A J^t \delta x_0.$$

Hence the d^2 matrix elements of Jacobian matrix satisfy the linearized equation (4.1)

$$\frac{d}{dt}J^i(x) = A(x)J^i(x), \quad \text{initial condition } J^0(x) = \mathbf{1}. \quad (4.9)$$

Given a numerical routine for integrating the equations of motion, evaluation of the Jacobian matrix requires minimal additional programming effort; one simply extends the d -dimensional integration routine and integrates concurrently with $f^i(x)$ the d^2 elements of $J^i(x)$.

The qualifier ‘simply’ is perhaps too glib. Integration will work for short finite times, but for exponentially unstable flows one quickly runs into numerical over- and/or underflow problems, so further thought will have to go into implementation this calculation.

So now we know how to compute Jacobian matrix J^i given the stability matrix A , at least when the d^2 extra equations are not too expensive to compute. Mission accomplished.



fast track:
chapter 7, p. 121

And yet... there are mopping up operations left to do. We persist until we derive the integral formula (4.43) for the Jacobian matrix, an analogue of the finite-time ‘Green function’ or ‘path integral’ solutions of other linear problems.

We are interested in smooth, differentiable flows. If a flow is smooth, in a sufficiently small neighborhood it is essentially linear. Hence the next section, which might seem an embarrassment (what is a section on *linear* flows doing in a book on *nonlinear* dynamics?), offers a firm stepping stone on the way to understanding nonlinear flows. If you know your eigenvalues and eigenvectors, you may prefer to fast forward here.



fast track:
sect. 4.3, p. 79

4.2 Linear flows

Diagonalizing the matrix: that’s the key to the whole thing.
— Governor Arnold Schwarzenegger

Linear fields are the simplest vector fields, described by linear differential equations which can be solved explicitly, with solutions that are good for all times.

The state space for linear differential equations is $\mathcal{M} = \mathbb{R}^d$, and the equations of motion (2.6) are written in terms of a vector x and a constant stability matrix A as

$$\dot{x} = v(x) = Ax. \quad (4.10)$$

Solving this equation means finding the state space trajectory

$$x(t) = (x_1(t), x_2(t), \dots, x_d(t))$$

passing through the point x_0 . If $x(t)$ is a solution with $x(0) = x_0$ and $y(t)$ another solution with $y(0) = y_0$, then the linear combination $ax(t) + by(t)$ with $a, b \in \mathbb{R}$ is also a solution, but now starting at the point $ax_0 + by_0$. At any instant in time, the space of solutions is a d -dimensional vector space, which means that one can find a basis of d linearly independent solutions.

How do we solve the linear differential equation (4.10)? If instead of a matrix equation we have a scalar one, $\dot{x} = \lambda x$, the solution is

$$x(t) = e^{t\lambda}x_0. \quad (4.11)$$

In order to solve the d -dimensional matrix case, it is helpful to rederive the solution (4.11) by studying what happens for a short time step δt . If at time $t = 0$ the position is $x(0)$, then

$$\frac{x(\delta t) - x(0)}{\delta t} = \lambda x(0), \quad (4.12)$$

which we iterate m times to obtain Euler’s formula for compounding interest

$$x(t) \approx \left(1 + \frac{t}{m}\lambda\right)^m x(0). \quad (4.13)$$

The term in parentheses acts on the initial condition $x(0)$ and evolves it to $x(t)$ by taking m small time steps $\delta t = t/m$. As $m \rightarrow \infty$, the term in parentheses converges to $e^{t\lambda}$. Consider now the matrix version of equation (4.12):

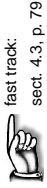
$$\frac{x(\delta t) - x(0)}{\delta t} = Ax(0). \quad (4.14)$$

A representative point x is now a vector in \mathbb{R}^d acted on by the matrix A , as in (4.10). Denoting by $\mathbf{1}$ the identity matrix, and repeating the steps (4.12) and (4.13) we obtain Euler’s formula for the exponential of a matrix:

$$x(t) = J^i x(0), \quad J^i = e^{tA} = \lim_{m \rightarrow \infty} \left(1 + \frac{t}{m}A\right)^m. \quad (4.15)$$

We will find this definition the exponential of a matrix helpful in the general case, where the matrix $A = A(x(t))$ varies along a trajectory.

How do we compute the exponential (4.15)?



fast track:
sect. 4.3, p. 79

Example 4.2 Jacobian matrix eigenvalues, diagonalizable case: Should we be so lucky that $A = A_D$ happens to be a diagonal matrix with eigenvalues $(\lambda^{(1)}, \lambda^{(2)}, \dots, \lambda^{(d)})$, the exponential is simply

$$J^t = e^{A_D t} = \begin{pmatrix} e^{\lambda^{(1)} t} & \dots & 0 \\ \vdots & \ddots & \vdots \\ 0 & \dots & e^{\lambda^{(d)} t} \end{pmatrix}. \quad (4.16)$$

Next, suppose that A is diagonalizable and that U is a nonsingular matrix that brings it to a diagonal form $A_D = U^{-1}AU$. Then J can also be brought to a diagonal form (insert factors $\mathbf{1} = UU^{-1}$ between the terms of the product (4.15)):

$$J^t = e^{At} = U e^{A_D t} U^{-1}. \quad (4.17)$$

The action of both A and J is very simple: the axes of orthogonal coordinate system where A is diagonal are also the eigen-directions of J^t , and under the flow the neighborhood is deformed by a multiplication by an eigenvalue factor for each coordinate axis.

In general J^t is neither diagonal, nor diagonalizable, nor constant along the trajectory. As any matrix, J^t can also be expressed in the singular value decomposition form

$$J = UDV^T \quad (4.18)$$

where D is diagonal, and U, V are orthogonal matrices. The diagonal elements $\sigma_1, \sigma_2, \dots, \sigma_d$ of D are called the *singular values* of J , namely the square root of the eigenvalues of $J^T J$, which is a symmetric, positive semi-definite matrix (and thus admits only real, non-negative eigenvalues). From a geometric point of view, when all singular values are non-zero, J maps the unit sphere into an ellipsoid: the singular values are then the lengths of the semiaxes of this ellipsoid.

Example 4.3 Singular values and geometry of deformations: Suppose we are in three dimensions, and J is not singular, so that the diagonal elements of D in (4.18) satisfy $\sigma_1 \geq \sigma_2 \geq \sigma_3 > 0$, and consider how J maps the unit ball $S = \{x \in \mathbb{R}^3 \mid x^2 = 1\}$. V is orthogonal (rotation/reflection), so $V^T S$ is still the unit sphere: then D maps S onto ellipsoid $\tilde{S} = \{y \in \mathbb{R}^3 \mid y_1^2/\sigma_1^2 + y_2^2/\sigma_2^2 + y_3^2/\sigma_3^2 = 1\}$ whose principal axes directions - y coordinates - are determined by V . Finally the ellipsoid is further rotated by the orthogonal matrix U . The local directions of stretching and their images under J are called the *right-hand* and *left-hand* singular vectors for J , and are given by the columns in V and U respectively: it is easy to check that $Jv_k = \sigma_k u_k$, if v_k, u_k are the k -th columns of V and U .

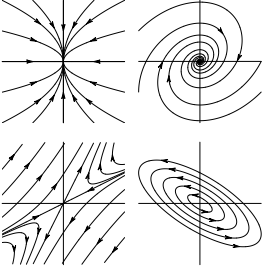


Figure 4.4: Streamlines for several typical 2-dimensional flows: saddle (hyperbolic), in node (attracting), center (elliptic), in spiral.

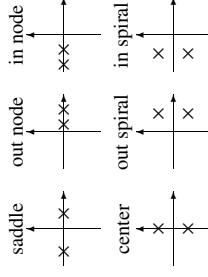


Figure 4.5: Qualitatively distinct types of eigenvalues of a [2x2] Jacobian matrix.

We recapitulate the basic facts of linear algebra in appendix B. A 2-dimensional example serves well to highlight the most important types of linear flows:

section 5.1.2

Example 4.4 Linear stability of 2-dimensional flows: For a 2-dimensional flow the eigenvalues $\lambda^{(1)}, \lambda^{(2)}$ of A are either real, leading to a linear motion along their eigenvectors, $x_j(t) = x_j(0) \exp(\lambda^{(j)} t)$, or a form a complex conjugate pair $\lambda^{(1)} = \mu + i\omega, \lambda^{(2)} = \mu - i\omega$, leading to a circular or spiral motion in the $[x_1, x_2]$ plane.

These two possibilities are refined further into sub-cases depending on the signs of the real part. In the case $\lambda^{(1)} > 0, \lambda^{(2)} < 0, x_1$ grows exponentially with time, and x_2 contracts exponentially. This behavior, called a saddle, is sketched in figure 4.4, as are the remaining possibilities: in/out nodes, inward/outward spirals, and the center. The magnitude of out-spiral $|x(t)|$ diverges exponentially when $\mu > 0$, and in-spiral contracts into $(0, 0)$ when the $\mu < 0$, whereas the phase velocity ω controls its oscillations.

If eigenvalues $\lambda^{(1)} = \lambda^{(2)} = \lambda$ are degenerate, the matrix might have two linearly independent eigenvectors, or only one eigenvector. We distinguish two cases: (a) A can be brought to diagonal form. (b) A can be brought to Jordan form, which (in dimension 2 or higher) has zeros everywhere except for the repeating eigenvalues on the diagonal, and some 1's directly above it. For every such Jordan $[d_k \times d_k]$ block there is only one eigenvector per block.

We sketch the full set of possibilities in figures 4.4 and 4.5, and work out in detail the most important cases in appendix B, example B.3.

4.2.1 Eigenvalues, multipliers - a notational interlude

Throughout this text the symbol Λ_k will always denote the k th *eigenvalue* (in literature sometimes referred to as the *multiplier* or *Floquet multiplier*) of the finite time Jacobian matrix J^t . Symbol $\lambda^{(k)}$ will be reserved for the k th *Floquet* or *characteristic* exponent, or *characteristic value*, with real part $\mu^{(k)}$ and phase $\omega^{(k)}$:

$$\Lambda_k = e^{\lambda^{(k)}} = e^{t(\mu^{(k)} + i\omega^{(k)})}. \quad (4.19)$$

$J^t(x_0)$ depends on the initial point x_0 and the elapsed time t . For notational brevity we tend to omit this dependence, but in general

$$\Lambda = \Lambda_k = \Lambda_k(x_0, t), \quad \lambda = \lambda^{(k)}(x_0, t), \quad \omega = \omega^{(k)}(x_0, t), \dots \text{ etc.},$$

depend on both the trajectory traversed and the choice of coordinates.

However, as we shall see in sect. 5.2, if the stability matrix A or the Jacobian matrix J is computed on a flow-invariant set \mathcal{M}_p , such as an equilibrium q or a periodic orbit p of period T_p ,

$$A_q = A(x_q), \quad J_p(x) = J^{T_p}(x), \quad x \in \mathcal{M}_p, \quad (4.20)$$

(x is any point on the cycle) its eigenvalues

$$\lambda_q^{(k)} = \lambda^{(k)}(x_q), \quad \Lambda_{p,k} = \Lambda_k(x, T_p)$$

are flow-invariant, independent of the choice of coordinates and the initial point in the cycle p , so we label them by their q or p label.

We number eigenvalues Λ_k in order of decreasing magnitude

$$|\Lambda_1| \geq |\Lambda_2| \geq \dots \geq |\Lambda_d|. \quad (4.21)$$

Since $|\Lambda_j| = e^{t\mu^{(j)}}$, this is the same as labeling by

$$\mu^{(1)} \geq \mu^{(2)} \geq \dots \geq \mu^{(d)}. \quad (4.22)$$

In dynamics the expanding directions, $|\Lambda_e| > 1$, have to be taken care of first, while the contracting directions $|\Lambda_c| < 1$ tend to take care of themselves, hence the ordering by decreasing magnitude is the natural one.



fast track:
sect. 4.3, p. 79

4.2.2 Yes, but how do you really do it?

Economical description of neighborhoods of equilibria and periodic orbits is afforded by projection operators

$$\mathbf{P}_i = \prod_{j \neq i} \frac{\mathbf{M} - \lambda^{(j)} \mathbf{1}}{\lambda^{(i)} - \lambda^{(j)}}, \quad (4.23)$$

where matrix \mathbf{M} is typically either equilibrium stability matrix A , or periodic orbit Jacobian matrix \hat{J} restricted to a Poincaré section, as in (4.56). While usually not phrased in language of projection operators, the requisite linear algebra is standard, and relegated here to appendix B.

Once the distinct non-zero eigenvalues $\{\lambda^{(i)}\}$ are computed, projection operators are polynomials in \mathbf{M} which need no further diagonalizations or orthogonalizations. For each distinct eigenvalue $\lambda^{(i)}$ of \mathbf{M} , the columns/rows of \mathbf{P}_i

$$(\mathbf{M} - \lambda^{(i)} \mathbf{1}) \mathbf{P}_j = \mathbf{P}_j (\mathbf{M} - \lambda^{(i)} \mathbf{1}) = 0, \quad (4.24)$$

are the right/left eigenvectors $\mathbf{e}^{(k)}$, $\mathbf{e}_{(k)}$ of \mathbf{M} which (provided \mathbf{M} is not of Jordan type) span the corresponding linearized subspace, and are a convenient starting seed for tracing out the global unstable/stable manifolds.

Matrices \mathbf{P}_i are *orthogonal* and *complete*:

$$\mathbf{P}_i \mathbf{P}_j = \delta_{ij} \mathbf{P}_j, \quad (\text{no sum on } j), \quad \sum_{i=1}^r \mathbf{P}_i = \mathbf{1}. \quad (4.25)$$

with the dimension of the i th subspace given by $d_i = \text{tr} \mathbf{P}_i$. Completeness relation substituted into $\mathbf{M} = \mathbf{M} \mathbf{1}$ yields

$$\mathbf{M} = \lambda^{(1)} \mathbf{P}_1 + \lambda^{(2)} \mathbf{P}_2 + \dots + \lambda^{(r)} \mathbf{P}_r. \quad (4.26)$$

As any matrix function $f(\mathbf{M})$ takes the scalar value $f(\lambda^{(i)})$ on the \mathbf{P}_i subspace, $f(\mathbf{M}) \mathbf{P}_i = f(\lambda^{(i)}) \mathbf{P}_i$, it is easily evaluated through its *spectral decomposition*

$$f(\mathbf{M}) = \sum_i f(\lambda^{(i)}) \mathbf{P}_i. \quad (4.27)$$

As \mathbf{M} has only real entries, it will in general have either real eigenvalues (over-damped oscillator, for example), or complex conjugate pairs of eigenvalues (under-damped oscillator, for example). That is not surprising, but also the corresponding eigenvectors can be either real or complex. All coordinates used in

defining the flow are real numbers, so what is the meaning of a *complex* eigenvector?

If two eigenvalues form a complex conjugate pair, $\{\lambda^{(k)}, \lambda^{(k+1)}\} = \{\mu + i\omega, \mu - i\omega\}$, they are in a sense degenerate: while a real $\lambda^{(k)}$ characterizes a motion along a line, a complex $\lambda^{(k)}$ characterizes a spiralling motion in a plane. We determine this plane by replacing the corresponding complex eigenvectors by their real and imaginary parts, $\{\mathbf{e}^{(k)}, \mathbf{e}^{(k+1)}\} \rightarrow \{\text{Re } \mathbf{e}^{(k)}, \text{Im } \mathbf{e}^{(k)}\}$, or, in terms of projection operators:

$$\mathbf{P}_k = \frac{1}{2}(\mathbf{R} + i\mathbf{Q}), \quad \mathbf{P}_{k+1} = \mathbf{P}_k^*,$$

where $\mathbf{R} = \mathbf{P}_k + \mathbf{P}_{k+1}$ is the subspace decomposed by the k th complex eigenvalue pair, and $\mathbf{Q} = (\mathbf{P}_k - \mathbf{P}_{k+1})/i$, both matrices with real elements. Substitution

$$\begin{pmatrix} \mathbf{P}_k \\ \mathbf{P}_{k+1} \end{pmatrix} = \frac{1}{2} \begin{pmatrix} 1 & i \\ 1 & -i \end{pmatrix} \begin{pmatrix} \mathbf{R} \\ \mathbf{Q} \end{pmatrix},$$

brings the $\lambda^{(k)}\mathbf{P}_k + \lambda^{(k+1)}\mathbf{P}_{k+1}$ complex eigenvalue pair in the spectral decomposition (4.26) into the real form,

$$(\mathbf{P}_k \quad \mathbf{P}_{k+1}) \begin{pmatrix} \lambda & 0 \\ 0 & \lambda^* \end{pmatrix} \begin{pmatrix} \mathbf{P}_k \\ \mathbf{P}_{k+1} \end{pmatrix} = (\mathbf{R} \quad \mathbf{Q}) \begin{pmatrix} \mu & -\omega \\ \omega & \mu \end{pmatrix} \begin{pmatrix} \mathbf{R} \\ \mathbf{Q} \end{pmatrix}, \quad (4.28)$$

where we have dropped the superscript (k) for notational brevity.

To summarize, spectrally decomposed matrix \mathbf{M} (4.26) acts along lines on subspaces corresponding to real eigenvalues, and as a $[2 \times 2]$ rotation in a plane on subspaces corresponding to complex eigenvalue pairs.

Now that we have some feeling for the qualitative behavior of eigenvectors and eigenvalues of linear flows, we are ready to return to the nonlinear case.

4.3 Stability of flows



How do you determine the eigenvalues of the finite time local deformation J^t for a general nonlinear smooth flow? The Jacobian matrix is computed by integrating the equations of variations (4.2)

$$\dot{x}(t) = f^t(x_0), \quad \delta x(x_0, t) = J^t(x_0) \delta x(x_0, 0). \quad (4.29)$$

The equations are linear, so we should be able to integrate them—but in order to make sense of the answer, we derive this integral step by step.

4.3.1 Stability of equilibria

For a start, consider the case where x is an equilibrium point (2.8). Expanding around the equilibrium point x_q , using the fact that the stability matrix $A = A(x_q)$ in (4.2) is constant, and integrating,

$$f^t(x) = x_q + e^{At}(x - x_q) + \dots, \quad (4.30)$$

we verify that the simple formula (4.15) applies also to the Jacobian matrix of an equilibrium point,

$$J^t(x_q) = e^{At}, \quad A_q = A(x_q). \quad (4.31)$$

Example 4.5 In-out spirals. Consider an equilibrium whose Floquet exponents $\{\lambda^{(1)}, \lambda^{(2)}\} = \{\mu + i\omega, \mu - i\omega\}$ form a complex conjugate pair. The corresponding complex eigenvectors can be replaced by their real and imaginary parts, $\{\mathbf{e}^{(1)}, \mathbf{e}^{(2)}\} \rightarrow \{\text{Re } \mathbf{e}^{(1)}, \text{Im } \mathbf{e}^{(1)}\}$. The 2-dimensional real representation (4.28),

$$\begin{pmatrix} \mu & -\omega \\ \omega & \mu \end{pmatrix} = \mu \begin{pmatrix} 1 & 0 \\ 0 & 1 \end{pmatrix} + \omega \begin{pmatrix} 0 & -1 \\ 1 & 0 \end{pmatrix}$$

consists of the identity and the generator of $SO(2)$ rotations in the $\{\text{Re } \mathbf{e}^{(1)}, \text{Im } \mathbf{e}^{(1)}\}$ plane. Trajectories $\mathbf{x}(t) = J^t \mathbf{x}(0)$, where (omitting $\mathbf{e}^{(3)}, \mathbf{e}^{(4)}, \dots$ eigen-directions)

$$J^t = e^{A_q t} = e^{\mu t} \begin{pmatrix} \cos \omega t & -\sin \omega t \\ \sin \omega t & \cos \omega t \end{pmatrix}, \quad (4.32)$$

spiral in/out around $(x, y) = (0, 0)$, see figure 4.4, with the rotation period T , and contraction/expansion radially by the multiplier Λ_{radial} , and by the multiplier Λ_j along the $\mathbf{e}^{(j)}$ eigen-direction per a turn of the spiral: exercise B.1

$$T = 2\pi/\omega, \quad \Lambda_{\text{radial}} = e^{\mu T}, \quad \Lambda_j = e^{T\mu^{(j)}}. \quad (4.33)$$

We learn that the typical turnover time scale in the neighborhood of the equilibrium $(x, y) = (0, 0)$ is of order $\approx T$ (and not, let us say, $1000T$, or $10^{-2}T$). Λ_j multipliers give us estimates of strange-set thickness in eigen-directions transverse to the rotation plane.

Example 4.6 Stability of equilibria of the Rössler flow. (continued from example 4.1) The Rössler system (2.17) has two equilibrium points (2.18), the inner equilibrium (x_-, y_-, z_-) , and the outer equilibrium point (x^+, y^+, z^+) . Together with exercise 2.8 exponents (eigenvalues of the stability matrix) the two equilibria yield quite detailed information about the flow. Figure 4.6 shows two trajectories which start in the neighborhood of the outer '+' equilibrium. Trajectories to the right of the equilibrium point '+' escape, and those to the left spiral toward the inner equilibrium point '-', where they seem to wander chaotically for all times. The stable manifold of outer equilibrium point thus serves as the attraction basin boundary. Consider now the numerical values for eigenvalues of the two equilibria

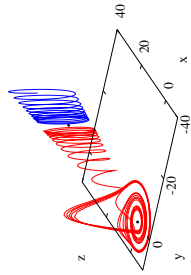


Figure 4.6: Two trajectories of the Rössler flow initiated in the neighborhood of the ‘+’ or ‘outer’ equilibrium point (2.18). (R. Paškauskas)

$$\begin{aligned} (\mu_+^{(1)}, \mu_+^{(2)} \pm i\omega_+^{(2)}) &= (-5.686, 0.0970 \pm i0.9951) \\ (\mu_+^{(1)}, \mu_+^{(2)} \pm i\omega_+^{(2)}) &= (0.1929, -4.596 \times 10^{-6} \pm i5.428) \end{aligned} \quad (4.34)$$

Outer equilibrium: The $\mu_+^{(2)} \pm i\omega_+^{(2)}$ complex eigenvalue pair implies that that neighborhood of the outer equilibrium point rotates with angular period $T_+ \approx |2\pi/\omega_+^{(2)}| = 1.1575$. The multiplier by which a trajectory that starts near the ‘+’ equilibrium point contracts in the stable manifold plane is the exorbitatingly slow $\Lambda_+^{(2)} \approx \exp(\mu_+^{(2)}T_+) = 0.9999947$ per rotation. For each period the point of the stable manifold moves away along the unstable eigen-direction by factor $\Lambda_+^{(1)} \approx \exp(\mu_+^{(1)}T_+) = 1.2497$. Hence the slow spiraling on both sides of the ‘+’ equilibrium point.

Inner equilibrium: The $\mu_-^{(2)} \pm i\omega_-^{(2)}$ complex eigenvalue pair tells us that neighborhood of the ‘-’ equilibrium point rotates with angular period $T_- \approx |2\pi/\omega_-^{(2)}| = 6.313$, slightly faster than the harmonic oscillator estimate in (2.14). The multiplier by which a trajectory that starts near the ‘-’ equilibrium point spirals away per one rotation is $\Lambda_-^{(1)} \approx \exp(\mu_-^{(1)}T_-) = 1.84$. The $\mu_-^{(1)}$ eigenvalue is essentially the z -expansion correcting parameter c introduced in (2.16). For each Poincaré section return, the trajectory is contracted into the stable manifold by the amazing factor of $\Lambda_1 \approx \exp(\mu_-^{(1)}T_-) = 10^{-15.6}$ (I).

Suppose you start with a 1 mm interval pointing in the Λ_1 eigen-direction. After one Poincaré return the interval is of order of 10^{-4} fermi, the furthest we will get into subnuclear structure in this book. Of course, from the mathematical point of view, the flow is reversible, and the Poincaré return map is invertible. (continued in example 11.3) (R. Paškauskas)

Example 4.7 Stability of Lorenz flow equilibria: (continued from example 4.1) A glance at figure 3.7 suggests that the flow is organized by its 3 equilibria, so lets have a closer look at their stable/unstable manifolds.

The E_{O_0} equilibrium stability matrix (4.4) evaluated at $x_{E_{O_0}} = (0, 0, 0)$ is block-diagonal. The z -axis is an eigenvector with a contracting eigenvalue $\lambda^{(3)} = -b$. From (4.48) it follows that all $[x, y]$ areas shrink at rate $-(\sigma + 1)$. Indeed, the $[x, y]$ submatrix

$$A^- = \begin{pmatrix} -\sigma & \sigma \\ \rho & -1 \end{pmatrix} \quad (4.35)$$

has a real expanding/contracting eigenvalue pair $\lambda^{(1,2)} = -(\sigma + 1)/2 \pm \sqrt{(\sigma - 1)^2/4 + \rho\sigma}$, with the right eigenvectors $e^{(1)}, e^{(2)}$ in the $[x, y]$ plane, given by (either) column of the projection operator

$$P_i = \frac{\Lambda^- - \lambda^{(j)}I}{\lambda^{(i)} - \lambda^{(j)}} = \frac{1}{\lambda^{(i)} - \lambda^{(j)}} \begin{pmatrix} -\sigma - \lambda^{(j)} & \sigma \\ \rho & -1 - \lambda^{(j)} \end{pmatrix}, \quad i \neq j \in \{1, 2\}. \quad (4.36)$$

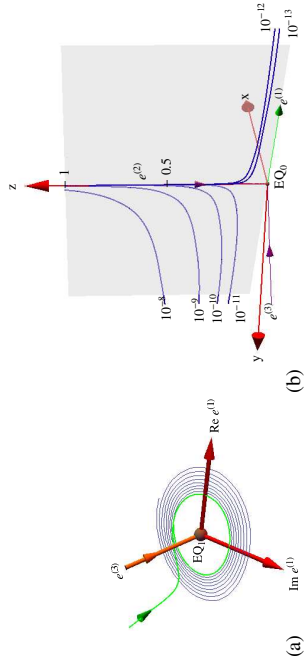


Figure 4.7: (a) A perspective view of the linearized Lorenz flow near E_{O_1} equilibrium, see figure 3.7 (a). The unstable eigenplane of E_{O_1} is spanned by $\text{Re } e^{(1)}$ and $\text{Im } e^{(1)}$. The stable eigenvector $e^{(3)}$. (b) Lorenz flow near the E_{O_0} equilibrium: unstable eigenvector $e^{(1)}$, stable eigenvectors $e^{(2)}, e^{(3)}$. Trajectories initiated at distances $10^{-9}, \dots, 10^{-12}, 10^{-15}$ away from the z -axis exit finite distance from E_{O_0} along the $(e^{(1)}, e^{(2)})$ eigen-vectors plane. Due to the strong $\Lambda^{(1)}$ expansion, the E_{O_0} equilibrium is, for all practical purposes, unreachable, and the $E_{O_1} \rightarrow E_{O_0}$ heteroclinic connection never observed in simulations such as figure 2.5. (E. Siminos; continued in figure 11.8.)

$E_{O_{1,2}}$ equilibria have no symmetry, so their eigenvalues are given by the roots of a cubic equation, the secular determinant $\det(\Lambda - \lambda I) = 0$:

$$\lambda^3 + \lambda^2(\sigma + b + 1) + \lambda b(\sigma + \rho) + 2\sigma b(\rho - 1) = 0. \quad (4.37)$$

For $\rho > 24.74$, $E_{O_{1,2}}$ have one stable real eigenvalue and one unstable complex conjugate pair, leading to a spiral-out instability and the strange attractor depicted in figure 2.5.

As all numerical plots of the Lorenz flow are here carried out for the Lorenz parameter choice $\sigma = 10, b = 8/3, \rho = 28$, we note the values of these eigenvalues for future reference,

$$\begin{aligned} E_{O_0} : (\lambda^{(1)}, \lambda^{(2)}, \lambda^{(3)}) &= (11.83, -2.666, -22.83) \\ E_{O_1} : (\mu^{(1)} \pm i\omega^{(1)}, \lambda^{(3)}) &= (0.094 \pm i10.19, -13.85), \end{aligned} \quad (4.38)$$

as well as the rotation period $T_{E_{O_0}} = 2\pi/\omega^{(1)}$ about E_{O_0} , and the associated expansion/contraction multipliers $\Lambda^{(i)} = \exp(\mu^{(i)}T_{E_{O_0}})$ per a spiral-out turn:

$$T_{E_{O_0}} = 0.6163, \quad (\Lambda^{(1)}, \Lambda^{(3)}) = (1.060, 1.957 \times 10^{-4}). \quad (4.39)$$

We learn that the typical turnover time scale in this problem is of order $T \approx T_{E_{O_0}} \approx 1$ (and not, let us say, 1000, or 10^{-2}). Combined with the contraction rate (4.48), this tells us that the Lorenz flow strongly contracts state space volumes, by factor of $\approx 10^{-4}$ per mean turnover time.

In the E_{O_0} neighborhood the unstable manifold trajectories slowly spiral out, with very small radial per-turn expansion multiplier $\Lambda^{(1)} \approx 1.06$, and very strong contraction multiplier $\Lambda^{(3)} \approx 10^{-4}$ onto the unstable manifold, figure 4.7 (a). This contraction confines, for all practical purposes, the Lorenz attractor to a 2-dimensional surface evident in the section figure 3.7.

In the $x_{E_{O_0}} = (0, 0, 0)$ equilibrium neighborhood the extremely strong $\lambda^{(3)} \approx -23$ contraction along the $e^{(3)}$ direction confines the hyperbolic dynamics near E_{O_0} to the plane spanned by the unstable eigenvector $e^{(1)}$, with $\lambda^{(1)} \approx 12$, and the slowest contraction rate eigenvector $e^{(2)}$ along the z -axis, with $\lambda^{(2)} \approx -3$. In this plane the strong expansion along $e^{(1)}$ overwhelms the slow $\lambda^{(2)} \approx -3$ contraction down the z -axis, making it extremely unlikely for a random trajectory to approach E_{O_0} , figure 4.7 (b). Thus linearization suffices to describe analytically the singular dip in the Poincaré sections of figure 3.7, and the empirical scarcity of trajectories close to E_{O_0} . (continued in example 4.9)

(E. Siminos and J. Halcrow)

Example 4.8 Lorenz flow: Global portrait. (continued from example 4.7) As the E_{Q_1} unstable manifold spirals out, the strip that starts out in the section above E_{Q_1} in figure 3.7 cuts across the z -axis invariant subspace. This strip necessarily contains a heteroclinic orbit that hits the z -axis head on, and in infinite time (but exponentially fast) descends all the way to E_{Q_0} .

How? As in the neighborhood of the E_{Q_0} equilibrium the dynamics is linear (see figure 4.7 (a)), there is no need to integrate numerically the final segment of the heteroclinic connection - it is sufficient to bring a trajectory a small distance away from E_{Q_0} , continue analytically to a small distance beyond E_{Q_0} , then resume the numerical integration.

What happens next? Trajectories to the left of z -axis shoot off along the $e^{(1)}$ direction, and those to the right along $-e^{(1)}$. As along the $e^{(1)}$ direction $xy > 0$, the nonlinear term in the z equation (2.12) bends both branches of the E_{Q_0} unstable manifold $W^u(E_{Q_0})$ upwards. Then ... - never mind. Best to postpone the completion of this narrative to example 9.10, where the discrete symmetry of Lorenz flow will help us streamline the analysis. As we shall show, what we already know about the 3 equilibria and their stable/unstable manifolds suffices to completely pin down the topology of Lorenz flow. (continued in example 9.10)

(E. Siminos and J. Halcrow)

4.3.2 Stability of trajectories

Next, consider the case of a general, non-stationary trajectory $x(t)$. The exponential of a constant matrix can be defined either by its Taylor series expansion, or in terms of the Euler limit (4.15):

$$e^{tA} = \sum_{k=0}^{\infty} \frac{t^k}{k!} A^k \quad (4.40)$$

$$= \lim_{m \rightarrow \infty} \left(\mathbf{1} + \frac{t}{m} A \right)^m \quad (4.41)$$

Taylor expanding is fine if A is a constant matrix. However, only the second, tax-accountant's discrete step definition of an exponential is appropriate for the task at hand, as for a dynamical system the local rate of neighborhood distortion $A(x)$ depends on where we are along the trajectory. The linearized neighborhood is multiplicatively deformed along the flow, and the m discrete time step approximation to J^t is therefore given by a generalization of the Euler product (4.41):

$$J^t = \lim_{m \rightarrow \infty} \prod_{n=m}^1 \left(\mathbf{1} + \delta t A(x_n) \right) = \lim_{m \rightarrow \infty} \prod_{n=m}^1 e^{\delta t A(x_n)} \quad (4.42)$$

$$= \lim_{m \rightarrow \infty} e^{\delta t A(x_m)} e^{\delta t A(x_{m-1})} \dots e^{\delta t A(x_2)} e^{\delta t A(x_1)},$$

where $\delta t = (t - t_0)/m$, and $x_n = x(t_0 + n\delta t)$. Slightly perverse indexing of the products indicates that the successive infinitesimal deformation are applied by

multiplying from the left. The two formulas for J^t agree to leading order in δt , and the $m \rightarrow \infty$ limit of this procedure is the integral

$$J_{ij}^t(x_0) = \left[\mathbf{T} e^{\int_0^t d\tau A(x(\tau))} \right]_{ij}, \quad (4.43)$$

where \mathbf{T} stands for time-ordered integration, defined as the continuum limit of the successive left multiplications (4.42). This integral formula for J is the main conceptual result of this chapter. exercise 4.5

It makes evident important properties of Jacobian matrices, such as that they are multiplicative along the flow,

$$J^{t+t'}(x) = J^{t'}(x') J^t(x), \quad \text{where } x' = f^{t'}(x), \quad (4.44)$$

an immediate consequence of time-ordered product structure of (4.42). However, in practice J is evaluated by integrating (4.9) along with the ODEs that define a particular flow.



in depth:
sect. 17.3, p. 340

4.4 Neighborhood volume



section 17.3
remark 17.3

Consider a small state space volume $\Delta V = d^d x$ centered around the point x_0 at time $t = 0$. The volume $\Delta V'$ around the point $x' = x(t)$ time t later is

$$\Delta V' = \frac{\Delta V'}{\Delta V} \Delta V = \left| \det \frac{\partial x'}{\partial x} \right| \Delta V = |\det J(x_0)^t| \Delta V, \quad (4.45)$$

so the $|\det J|$ is the ratio of the initial and the final volumes. The determinant $\det J^t(x_0) = \prod_{i=1}^d \Lambda_i(x_0, t)$ is the product of the Floquet multipliers. We shall refer to this determinant as the *Jacobian* of the flow. This Jacobian is easily evaluated. exercise 4.1
Take the time derivative, use the J evolution equation (4.9) and the matrix identity $\ln \det J = \text{tr} \ln J$:

$$\frac{d}{dt} \ln \Delta V(t) = \frac{d}{dt} \ln \det J = \text{tr} \frac{d}{dt} \ln J = \text{tr} \frac{1}{J} \dot{J} = \text{tr} A = \partial_i v_i.$$

(Here, as elsewhere in this book, a repeated index implies summation.) Integrate both sides to obtain the time evolution of an infinitesimal volume

$$\det J^t(x_0) = \exp \left[\int_0^t d\tau \text{tr} \mathbf{A}(x(\tau)) \right] = \exp \left[\int_0^t d\tau \partial_i v_i(x(\tau)) \right]. \quad (4.46)$$

As the divergence $\partial_i v_i$ is a scalar quantity, the integral in the exponent (4.43) needs *no time ordering*. So all we need to do is evaluate the time average

$$\begin{aligned} \overline{\partial_i v_i} &= \lim_{t \rightarrow \infty} \frac{1}{t} \int_0^t d\tau \sum_{i=1}^d A_{ii}(x(\tau)) \\ &= \frac{1}{t} \ln \left| \prod_{i=1}^d \Lambda_i(x_0, t) \right| = \sum_{i=1}^d \lambda^{(i)}(x_0, t) \end{aligned} \quad (4.47)$$

along the trajectory. If the flow is not singular (for example, the trajectory does not run head-on into the Coulomb $1/r$ singularity), the stability matrix elements are bounded everywhere, $|A_{ij}| < M$, and so is the trace $\sum_i A_{ii}$. The time integral in (4.46) grows at most linearly with t , hence $\overline{\partial_i v_i}$ is bounded for all times, and numerical estimates of the $t \rightarrow \infty$ limit in (4.47) are not marred by any blowups.

Example 4.9 Lorenz flow state space contraction: (continued from example 4.7) It follows from (4.4) and (4.47) that Lorenz flow is volume contracting,

$$\partial_i v_i = \sum_{i=1}^3 \lambda^{(i)}(x, t) = -\sigma - b - 1, \quad (4.48)$$

at a constant, coordinate- and ρ -independent rate, set by Lorenz to $\partial_i v_i = -13.66$. As for periodic orbits and for long time averages there is no contraction/expansion along the flow, $\lambda^{(0)} = 0$, and the sum of $\lambda^{(i)}$ is constant by (4.48), there is only one independent exponent $\lambda^{(i)}$ to compute. (continued in example 4.8)

Even if we were to insist on extracting $\overline{\partial_i v_i}$ from (4.42) by first multiplying Jacobian matrices along the flow, and then taking the logarithm, we can avoid exponential blowups in J^t by using the multiplicative structure (4.44), $\det J^{t+t'}(x_0) = \det J^t(x') \det J^{t'}(x_0)$ to restart with $J^0(x') = \mathbf{1}$ whenever the eigenvalues of $J^t(x_0)$ start getting out of hand. In numerical evaluations of Lyapunov exponents, $\lambda_i = \lim_{t \rightarrow \infty} \mu^{(i)}(x_0, t)$, the sum rule (4.47) can serve as a helpful check on the accuracy of the computation. section 17.3

The divergence $\partial_i v_i$ characterizes the behavior of a state space volume in the infinitesimal neighborhood of the trajectory. If $\partial_i v_i < 0$, the flow is *locally contracting*, and the trajectory might be falling into an attractor. If $\partial_i v_i(x) < 0$, for all $x \in \mathcal{M}$, the flow is *globally contracting*, and the dimension of the attractor is necessarily smaller than the dimension of state space \mathcal{M} . If $\partial_i v_i = 0$, the flow preserves state space volume and $\det J^t = \mathbf{1}$. A flow with this property is called *incompressible*. An important class of such flows are the Hamiltonian flows considered in sect. 7.2.

But before we can get to that, Henri Roux, the perfect student and always alert, pipes up. He does not like our definition of the Jacobian matrix in terms of the time-ordered exponential (4.43). Depending on the signs of multipliers, the left hand side of (4.46) can be either positive or negative. But the right hand side is an exponential of a real number, and that can only be positive. What gives? As we shall see much later on in this text, in discussion of topological indices arising in semiclassical quantization, this is not at all a dumb question.

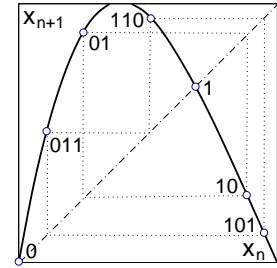


Figure 4.8: A unimodal map, together with fixed points $0, 1$, 2-cycle 01 and 3-cycle 011 .

4.5 Stability of maps



The transformation of an infinitesimal neighborhood of a trajectory under the iteration of a map follows from Taylor expanding the iterated mapping at finite time n to linear order, as in (4.5). The linearized neighborhood is transported by the Jacobian matrix evaluated at a discrete set of times $n = 1, 2, \dots$,

$$M_{ij}^n(x_0) = \left. \frac{\partial f_i^n(x)}{\partial x_j} \right|_{x=x_0}. \quad (4.49)$$

In case of a periodic orbit, $f^n(x) = x$, we shall refer to this Jacobian matrix as the *monodromy* matrix. Derivative notation $M^t(x_0) \rightarrow Df^t(x_0)$ is frequently employed in the literature. As in the continuous case, we denote by Λ_k the k th *eigenvalue* or multiplier of the finite time Jacobian matrix $M^n(x_0)$, and by $\mu^{(k)}$ the real part of k th *eigen-exponent*

$$\Lambda_{\pm} = e^{n(\mu \pm i\omega)}, \quad |\Lambda| = e^{n\mu}.$$

For complex eigenvalue pairs the phase ω describes the rotation velocity in the plane defined by the corresponding pair of eigenvectors, with one period of rotation given by

$$T = 2\pi/\omega. \quad (4.50)$$

Example 4.10 Stability of a 1-dimensional map: Consider the orbit $\{\dots, x_{n-1}, x_n, x_{n+1}, x_{n+2}, \dots\}$ of a 1-dimensional map $x_{n+1} = f(x_n)$. Since point x_n is carried into point x_{n+1} , in studying linear stability (and higher derivatives) of the map it is often convenient to deploy a local coordinate systems z_a centered on the orbit points x_a , together with a notation for the map, its derivative, and, by the chain rule, the derivative of the k th iterate f^k evaluated at the point x_a ,

$$\begin{aligned} x &= x_a + z_a, & f_a(z_a) &= f(x_a + z_a) \\ f'_a &= f'(x_a) \\ \Lambda(x_0, k) &= f_a^{k'} = f'_{a+k-1} \cdots f'_{a+1} f'_a, & k &\geq 2. \end{aligned} \quad (4.51)$$

Here a is the label of point x_a , and the label $a+1$ is a shorthand for the next point b on the orbit of x_a , $x_b = x_{a+1} = f(x_a)$. For example, a period-3 periodic point in figure 4.8 might have label $a = 011$, and by $x_{110} = f(x_{011})$ the next point label is $b = 110$.

The 1-step product formula for the stability of the n th iterate of a d -dimensional map

$$\begin{aligned} M^n(x_0) &= M(x_{n-1}) \cdots M(x_1)M(x_0), \\ M(x)_{kl} &= \frac{\partial}{\partial x_l} f_k(x), \quad x_m = f^m(x_0) \end{aligned} \quad (4.52)$$

follows from the chain rule for matrix derivatives

$$\frac{\partial}{\partial x_i} f_j(f(x)) = \sum_{k=1}^d \frac{\partial}{\partial y_k} f_j(y) \Big|_{y=f(x)} \frac{\partial}{\partial x_i} f_k(x).$$

If you prefer to think of a discrete time dynamics as a sequence of Poincaré section returns, then (4.52) follows from (4.44): Jacobian matrices are multiplicative along the flow. exercise 17.1


Example 4.11 Hénon map Jacobian matrix: For the Hénon map (3.19) the Jacobian matrix for the n th iterate of the map is

$$M^n(x_0) = \prod_{m=n}^1 \begin{pmatrix} -2ax_m & b \\ 1 & 0 \end{pmatrix}, \quad x_m = f_1^m(x_0, y_0). \quad (4.53)$$

The determinant of the Hénon one time step Jacobian matrix (4.53) is constant,

$$\det M = \Lambda_1 \Lambda_2 = -b \quad (4.54)$$

so in this case only one eigenvalue $\Lambda_1 = -b/\Lambda_2$ needs to be determined. This is not an accident; a constant Jacobian was one of desiderata that led Hénon to construct a map of this particular form.

 fast track:
chapter 7, p. 121

4.5.1 Stability of Poincaré return maps

(R. Paškauskas and P. Cvitanović)



We now relate the linear stability of the Poincaré return map $P : \mathcal{P} \rightarrow \mathcal{P}$ defined in sect. 3.1 to the stability of the continuous time flow in the full state space.

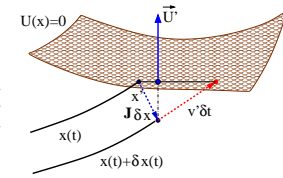


Figure 4.9: If $x(t)$ intersects the Poincaré section \mathcal{P} at time τ , the nearby $x(t) + \delta x(t)$ trajectory intersects it time $\tau + \delta \tau$ later. As $(U' \cdot v' \delta \tau) = -(U' \cdot J \delta x)$, the difference in arrival times is given by $\delta \tau = -(U' \cdot J \delta x)/(U' \cdot v')$.

The hypersurface \mathcal{P} can be specified implicitly through a function $U(x)$ that is zero whenever a point x is on the Poincaré section. A nearby point $x + \delta x$ is in the hypersurface \mathcal{P} if $U(x + \delta x) = 0$, and the same is true for variations around the first return point $x' = x(\tau)$, so expanding $U(x')$ to linear order in variation δx restricted to the Poincaré section leads to the condition

$$\sum_{i=1}^{d+1} \frac{\partial U(x')}{\partial x_i} \frac{dx'_i}{dx_j} \Big|_{\mathcal{P}} = 0. \quad (4.55)$$

In what follows $U_i = \partial_i U$ is the gradient of U defined in (3.3), unprimed quantities refer to the starting point $x = x_0 \in \mathcal{P}$, $v = v(x_0)$, and the primed quantities to the first return: $x' = x(\tau)$, $v' = v(x')$, $U' = U(x')$. For brevity we shall also denote the full state space Jacobian matrix at the first return by $J = J^\tau(x_0)$. Both the first return x' and the time of flight to the next Poincaré section $\tau(x)$ depend on the starting point x , so the Jacobian matrix

$$\hat{J}(x)_{ij} = \frac{dx'_i}{dx_j} \Big|_{\mathcal{P}} \quad (4.56)$$

with both initial and the final variation constrained to the Poincaré section hypersurface \mathcal{P} is related to the continuous flow Jacobian matrix by

$$\frac{dx'_i}{dx_j} \Big|_{\mathcal{P}} = \frac{\partial x'_i}{\partial x_j} + \frac{dx'_i}{d\tau} \frac{d\tau}{dx_j} = J_{ij} + v'_i \frac{d\tau}{dx_j}.$$

The return time variation $d\tau/dx$, figure 4.9, is eliminated by substituting this expression into the constraint (4.55),

$$0 = \partial_i U' J_{ij} + (v' \cdot \partial U') \frac{d\tau}{dx_j},$$

yielding the projection of the full space $(d+1)$ -dimensional Jacobian matrix to the Poincaré map d -dimensional Jacobian matrix:

$$\hat{J}_{ij} = \left(\delta_{ik} - \frac{v'_i \partial_k U'}{(v' \cdot \partial U')} \right) J_{kj}. \quad (4.57)$$

Substituting (4.7) we verify that the initial velocity $v(x)$ is a zero-eigenvector of \hat{J}

$$\hat{J}v = 0, \quad (4.58)$$

so the Poincaré section eliminates variations parallel to v , and \hat{J} is a rank d matrix, i.e., one less than the dimension of the continuous time flow.

Résumé

A neighborhood of a trajectory deforms as it is transported by a flow. In the linear approximation, the stability matrix A describes the shearing/compression/expansion of an infinitesimal neighborhood in an infinitesimal time step. The deformation after a finite time t is described by the Jacobian matrix

$$J^t(x_0) = \mathbf{T} e^{\int_0^t d\tau A(x(\tau))},$$

where \mathbf{T} stands for the time-ordered integration, defined multiplicatively along the trajectory. For discrete time maps this is multiplication by time step Jacobian matrix M along the n points $x_0, x_1, x_2, \dots, x_{n-1}$ on the trajectory of x_0 ,

$$M^n(x_0) = M(x_{n-1})M(x_{n-2}) \cdots M(x_1)M(x_0),$$

with $M(x)$ the single discrete time step Jacobian matrix. In ChaosBook Λ_k denotes the k th *eigenvalue* of the finite time Jacobian matrix $J^t(x_0)$, and $\mu^{(k)}$ the real part of k th *eigen-exponent*

$$|\Lambda| = e^{n\mu}, \quad \Lambda_{\pm} = e^{n(\mu \pm i\omega)}.$$

For complex eigenvalue pairs the ‘angular velocity’ ω describes rotational motion in the plane spanned by the real and imaginary parts of the corresponding pair of eigenvectors.

The eigenvalues and eigen-directions of the Jacobian matrix describe the deformation of an initial infinitesimal cloud of neighboring trajectories into a distorted cloud a finite time t later. Nearby trajectories separate exponentially along unstable eigen-directions, approach each other along stable directions, and change slowly (algebraically) their distance along marginal directions. The Jacobian matrix J^t is in general neither symmetric, nor diagonalizable by a rotation, nor do its (left or right) eigenvectors define an orthonormal coordinate frame. Furthermore, although the Jacobian matrices are multiplicative along the flow, in dimensions higher than one their eigenvalues in general are not. This lack of multiplicativity has important repercussions for both classical and quantum dynamics.

Commentary

Remark 4.1 Linear fbws. The subject of linear algebra generates innumerable tomes of its own; in sect. 4.2 we only sketch, and in appendix B recapitulate a few facts that our narrative relies on: a useful reference book is [4.1]. The basic facts are presented at length in many textbooks. The standard references that exhaustively enumerate and explain all possible cases are Hirsch and Smale [4.2] and Arnold [4.3]. A quick overview is given by Izhikevich [4.4]; for different notions of orbit stability see Holmes and Shea-Brown [4.5]. For ChaosBook purposes, we enjoyed the discussion in chapter 2 Meiss [4.6], chapter 1 of Perko [4.7] and chapters 3 and 5 of Glendinning [4.8] the most.

The construction of projection operators given here is taken from refs. [4.9, 4.10]. Who wrote this down first we do not know, lineage certainly goes all the way back to Lagrange polynomials [4.11], but projection operators tend to get drowned in sea of algebraic details. Halmos [4.12] is a good early reference - but we like Harter’s exposition [4.13, 4.14, 4.15] best, for its multitude of specific examples and physical illustrations.

The nomenclature tends to be a bit confusing. In referring to velocity gradients matrix A defined in (4.3) as the ‘stability matrix’ we follow Tabor [4.16]. Sometimes A , which describes the instantaneous shear of the trajectory point $x(x_0, t)$ is referred to as the ‘Jacobian matrix,’ a particularly unfortunate usage when one considers linearized stability of an equilibrium point (4.31). What Jacobi had in mind in his 1841 fundamental paper [4.17] on the determinants today known as ‘jacobians’ were transformations between different coordinate frames. These are dimensionless quantities, while dimensionally A_{ij} is 1/[time]. More unfortunate still is referring to $J^t = e^{tA}$ as an ‘evolution operator,’ which here (see sect. 17.2) refers to something altogether different. In this book Jacobian matrix J^t always refers to (4.6), the linearized deformation after a finite time t , either for a continuous time flow, or a discrete time mapping.

Remark 4.2 Matrix decompositions of Jacobian matrix. Though singular values decomposition provides geometrical insights into how tangent dynamics acts, many popular algorithms for asymptotic stability analysis (recovering Lyapunov spectrum) employ another standard matrix decomposition: the QR scheme [4.1], through which a nonsingular matrix A is (uniquely) written as a product of an orthogonal and an upper triangular matrix $A = QR$. This can be thought as a Gram-Schmidt decomposition of the column vectors of A (which are linearly independent as A is nonsingular). The geometric meaning of QR decomposition is that the volume of the d -dimensional parallelepiped spanned by the column vectors of A has a volume coinciding with the product of the diagonal elements of the triangular matrix R , whose role is thus pivotal in algorithms computing Lyapunov spectra [4.20, 4.21, 4.22].

Remark 4.3 Routh-Hurwitz criterion for stability of a fixed point. For a criterion that matrix has roots with negative real parts, see Routh-Hurwitz criterion [4.18, 4.19] on the coefficients of the characteristic polynomial. The criterion provides a necessary condition that a fixed point is stable, and determines the numbers of stable/unstable eigenvalues of a fixed point.

Exercises

- 4.1. **Trace-log of a matrix.** Prove that

$$\det M = e^{\text{Tr} \ln M},$$

for an arbitrary nonsingular finite dimensional matrix M , $\det M \neq 0$.

- 4.2. **Stability, diagonal case.** Verify the relation (4.17)

$$J^t = e^{tA} = \mathbf{U}^{-1} e^{tA_D} \mathbf{U}, \quad A_D = \mathbf{U} \mathbf{A} \mathbf{U}^{-1}.$$

- 4.3. **State space volume contraction.**

- Compute the Rössler flow volume contraction rate at the equilibria.
- Study numerically the instantaneous $\partial_i v_i$ along a typical trajectory on the Rössler attractor; color-code the points on the trajectory by the sign (and perhaps the magnitude) of $\partial_i v_i$. If you see regions of local expansion, explain them.
- (optional) color-code the points on the trajectory by the sign (and perhaps the magnitude) of $\partial_i v_i - \bar{\partial}_i v_i$.
- Compute numerically the average contraction rate (4.47) along a typical trajectory on the Rössler attractor. Plot it as a function of time.
- Argue on basis of your results that this attractor is of dimension smaller than the state space $d = 3$.
- (optional) Start some trajectories on the escape side of the outer equilibrium, color-code the points on the trajectory. Is the flow volume contracting?

(continued in exercise 20.12)

- 4.4. **Topology of the Rössler flow.** (continuation of exercise 3.1)

- Show that equation $|\det(A - \lambda \mathbf{1})| = 0$ for Rössler flow in the notation of exercise 2.8 can be written as

$$\lambda^3 + \lambda^2 c (p^{\bar{x}} - \epsilon) + \lambda (p^{\bar{x}} / \epsilon + 1 - c^2 \epsilon p^{\bar{x}}) \mp c \sqrt{D} = 0 \quad (4.59)$$

- Solve (4.59) for eigenvalues λ^{\pm} for each equilibrium as an expansion in powers of ϵ . Derive

$$\begin{aligned} \lambda_1^{\pm} &= -c + \epsilon c / (c^2 + 1) + o(\epsilon) \\ \lambda_2^{\pm} &= \epsilon c^3 / [2(c^2 + 1)] + o(\epsilon^2) \\ \theta_2^{\pm} &= 1 + \epsilon / [2(c^2 + 1)] + o(\epsilon) \\ \lambda_1^{\mp} &= c\epsilon(1 - \epsilon) + o(\epsilon^3) \\ \lambda_2^{\mp} &= -\epsilon^3 c^2 / 2 + o(\epsilon^6) \\ \theta_2^{\mp} &= \sqrt{1 + 1/\epsilon} (1 + o(\epsilon)) \end{aligned} \quad (4.60)$$

Compare with exact eigenvalues. What are dynamical implications of the extravagant value of λ_1^{\mp} ? (continued as exercise 13.10)

(R. Paškauskas)

- 4.5. **Time-ordered exponentials.** Given a time dependent matrix $V(t)$ check that the time-ordered exponential

$$\mathcal{U}(t) = \mathbf{T} e^{\int_0^t d\tau V(\tau)}$$

may be written as

$$\mathcal{U}(t) = \sum_{m=0}^{\infty} \int_0^t dt_1 \int_0^{t_1} dt_2 \cdots \int_0^{t_{m-1}} dt_m V(t_1) \cdots V(t_m)$$

and verify, by using this representation, that $\mathcal{U}(t)$ satisfies the equation

$$\dot{\mathcal{U}}(t) = V(t)\mathcal{U}(t),$$

with the initial condition $\mathcal{U}(0) = 1$.

- 4.6. **A contracting baker's map.** Consider a contracting (or 'dissipative') baker's map, acting on a unit square $[0, 1]^2 = [0, 1] \times [0, 1]$, defined by

$$\begin{pmatrix} x_{n+1} \\ y_{n+1} \end{pmatrix} = \begin{pmatrix} x_n/3 \\ 2y_n \end{pmatrix} \quad y_n \leq 1/2$$

$$\begin{pmatrix} x_{n+1} \\ y_{n+1} \end{pmatrix} = \begin{pmatrix} x_n/3 + 1/2 \\ 2y_n - 1 \end{pmatrix} \quad y_n > 1/2.$$

This map shrinks strips by a factor of 1/3 in the x -direction, and then stretches (and folds) them by a factor of 2 in the y -direction.

By how much does the state space volume contract for one iteration of the map?

References

- [4.1] C.D. Meyer, *Matrix Analysis and Applied Linear Algebra*, (SIAM, Philadelphia 2001).
- [4.2] M. W. Hirsch and S. Smale, *Differential Equations, Dynamical Systems, and Linear Algebra*, (Academic Press, San Diego 1974).
- [4.3] V.I. Arnold, *Ordinary Differential Equations*, (Mit Press, Cambridge 1978).
- [4.4] E. M. Izhikevich, "Equilibrium," www.scholarpedia.org/article/Equilibrium.
- [4.5] P. Holmes and E. T. Shea-Brown, "Stability," www.scholarpedia.org/article/Stability.
- [4.6] J. D. Meiss, *Differential Dynamical Systems* (SIAM, Philadelphia 2007).
- [4.7] L. Perko, *Differential Equations and Dynamical Systems* (Springer-Verlag, New York 1991).
- [4.8] P. Glendinning, *Stability, Instability, and Chaos* (Cambridge Univ. Press, Cambridge 1994).
- [4.9] P. Cvitanović, "Group theory for Feynman diagrams in non-Abelian gauge theories," *Phys. Rev. D* **14**, 1536 (1976).
- [4.10] P. Cvitanović, "Classical and exceptional Lie algebras as invariance algebras," Oxford preprint 40/77 (June 1977, unpublished); available on ChaosBook.org/refs.
- [4.11] K. Hoffman and R. Kunze, *Linear Algebra* (Prentice-Hall, Englewood Cliffs, NJ 1971), Chapter 6.
- [4.12] P. R. Halmos, *Finite-dimensional vector spaces* (D. Van Nostrand, Princeton, 1958).
- [4.13] W. G. Harter, *J. Math. Phys.* **10**, 4 (1969).
- [4.14] W. G. Harter and N. Dos Santos, "Double-group theory on the half-shell and the two-level system. I. Rotation and half-integral spin states," *Am. J. Phys.* **46**, 251 (1978).
- [4.15] W. G. Harter, *Principles of Symmetry, Dynamics, and Spectroscopy* (Wiley, New York 1974).
- [4.16] M. Tabor, Sect 1.4 "Linear stability analysis," in *Chaos and Integrability in Nonlinear Dynamics: An Introduction* (Wiley, New York 1989), pp. 20-31.
- [4.17] C. G. J. Jacobi, "De functionibus alternantibus earumque divisione per productum e differentii elementorum conflatum," in *Collected Works*, Vol. 22, 439; *J. Reine Angew. Math. (Crelle)* (1841).
- [4.18] wikipedia.org, "Routh-Hurwitz stability criterion."